**Supporting Information**

A switchable wettability surface with chemical stability and antifouling property for controllable oil-water separation

Hanpeng Gao, [†] Yan Liu,[*,†] *Guoyong Wang,[‡] Shuyi Li, [†] Zhiwu Han, [†] and Luquan Ren[†]*

[†]Key Laboratory of Bionic Engineering (Ministry of Education), Jilin University, Changchun 130022, P. R. China

[‡]Key Laboratory of Automobile Materials (Ministry of Education) and College of Materials Science and Engineering, Jilin University, Changchun, 130022, P. R. China
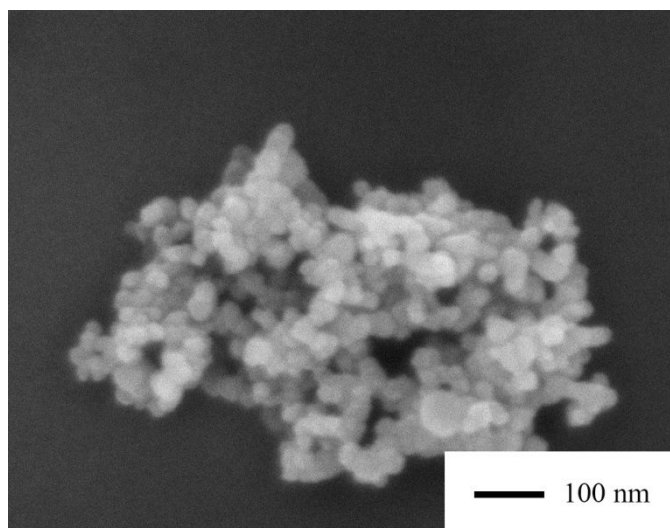
Figure S1. FE-SEM images of the nano TiO_2 particles.

Nano TiO_2 particles was first dissolved in alcohol and then dispersed by ultrasound. The mixed liquid was dropped on a silicon wafer and dried with N_2. The surface morphologies of TiO_2 were examined by using field emission scanning electron microscope (JSM-6700F, JEOL, Japan).


Figure S2. After 70 minutes of UV irradiation, the water contact angles of the BTTM was ~ 0 °.
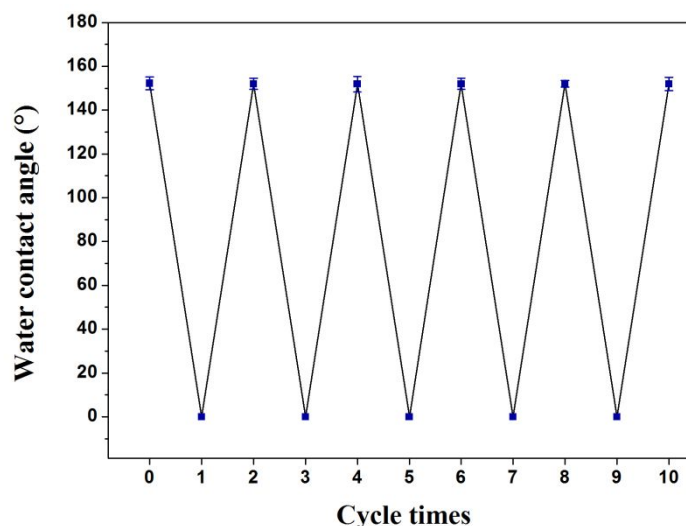
Figure S3. Reversible transformation between superhydrophobicity and superhydrophilicity realized by altering the UV irradiation and heating.

The changes in the surface hydroxyl content are considered to be the cause of the wettability transition. Here, the wettability relationship between the water droplets and the underwater oil droplets is further analyzed. For the original BTTM, due to the superhydrophobic character, it is very difficult to wet the surface in water, which makes the underwater oil droplet (the density of oil is greater than water) in full contact with the solid surface, resulting in underwater superoleophilicity. However, after UV irradiation, due to the superhydrophilicity, water can be trapped easily in the micro-nanostructures structure and formed a water film on the surface. As a consequence, a repellent force between nonpolar oil phase and the water-trapped polar surface was formed, which decreased the effective contact area between the solid surface and oil, causing underwater superoleophobicity. Therefore, the as-prepared surface has reversible switchable wettability.
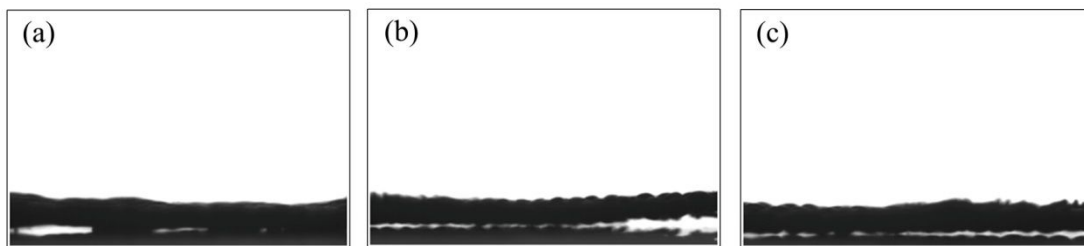
Figure S4. (a) The oil droplet contact angle of the original BTTM was ~ 0 °. (b) After UV irradiation, the as-prepared surface oil droplet contact angle was ~ 0 °. (c) After UV irradiation and followed by heating, the as-prepared surface oil droplet contact angle was still ~ 0 °.
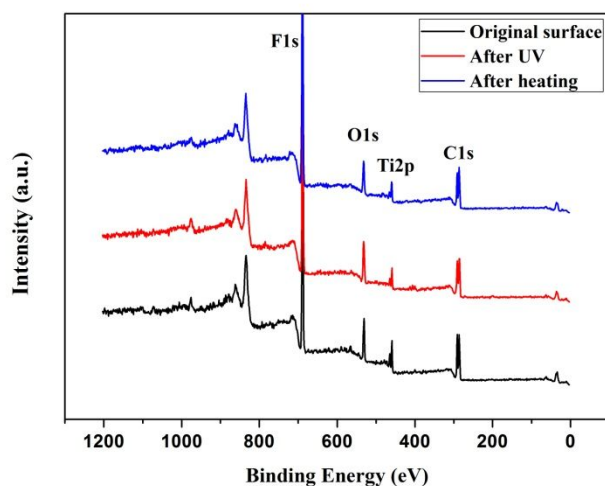

Figure S5. XPS survey spectra of original BTTM (black), after UV irradiation (red) and followed by heating (blue), respectively.

Table S1. The water contact angles (WCAs) and sliding angles (WSAs) of the BTTM (H_2O as reference).

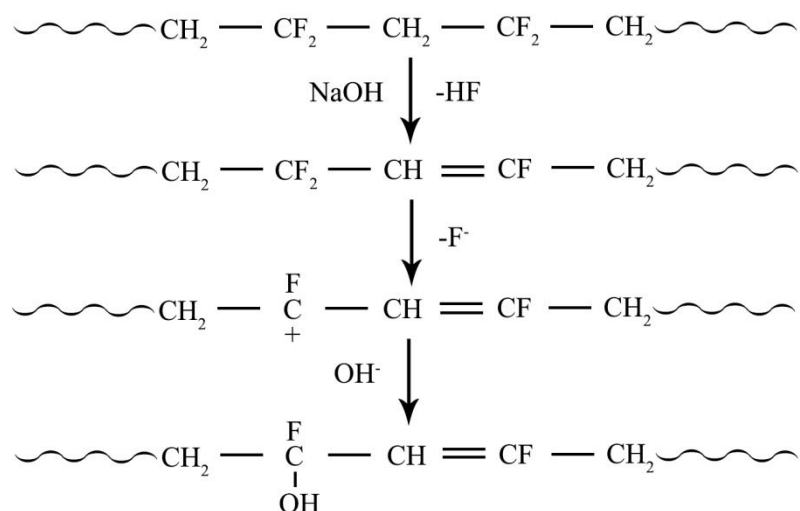|	WCAs	WSAs
H_2O	152.3 ± 3°	7.5 ± 3°
2 M HCl	151.7 ± 2°	7.3 ± 2.5°
2 M NaOH	150.7 ± 1.5°	12.5 ± 4.5°
2 M NaCl	152.0 ± 2.5°	7.5 ± 2°

Table S2. The underwater oil contact angles (UOCAs) and underwater oil sliding angles (UOSAs) of the BTTM (H_2O as reference).

	UOCAs	UOSAs
H_2O	151.6 ± 3°	6.3 ± 3°
2 M HCl	151.4 ± 1.5°	6.2 ± 2.5°
2 M NaOH	150.6 ± 2°	9.5 ± 3°
2 M NaCl	151.5 ± 2.5°	6.5 ± 2°
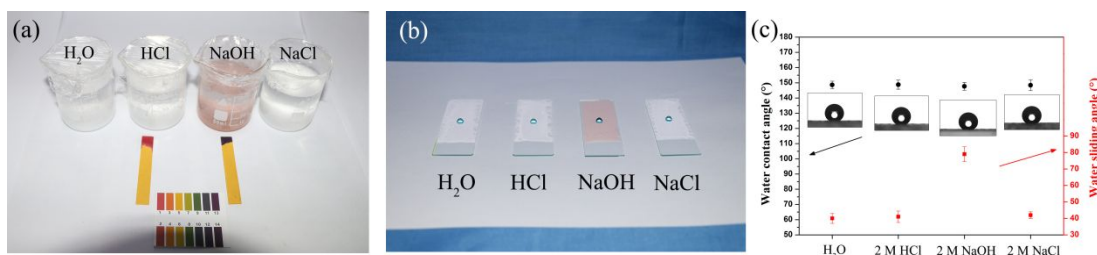
Figure S6. (a) PVDF was immersed in acid (HCl, 2 mol/L), alkali (NaOH, 2 mol/L) and salt solutions (NaCl, 2 mol/L) for 12 hours. (b) After immersing in different solutions for 12 hours, PVDF was coated on a glass substrate, and the water droplets remained spherical on the surface. (c) The WCAs and WSAs of the coated glass as a function of the different solutions (H_2O as reference).

It is well known that PVDF has good chemical stability as a low surface energy material. As shown in **Figure S6**a, PVDF was wetted by alcohol and immersed in different solutions. The color of PVDF changed in alkaline solution (NaOH, 2 mol/L) after 12 hours of immersion. It can be attributed to the alkali treatment leading to dehydrofluorination of PVDF (**Figure S7**). The color of the PVDF immersed in the other solution did not change. After immersing for 12 hours, the PVDF powder was rinsed repeatedly with deionized water and coated on glass. It can be observed that the water droplets still appear spherical on the surface (**Figure S6**b). The WCAs and WSAs of the glass substrate coated with different PVDF were measured (**Figure S6**c, **Table S3**). The results showed that PVDF immersed in acid and salt had little effect on wettability, while immersion in alkali caused an increase in WSAs. A similar experiment was performed on the BTTM.

$$\sim\sim CH_2 \text{---} CF_2 \text{---} CH_2 \text{---} CF_2 \text{---} CH_2 \sim\sim$$

$$\text{NaOH} \downarrow \text{-HF}$$

$$\sim\sim CH_2 \text{---} CF_2 \text{---} CH = CF \text{---} CH_2 \sim\sim$$

$$\downarrow \text{-F}^-$$

$$\sim\sim CH_2 \text{---} \overset{F}{\underset{+}{C}} \text{---} CH = CF \text{---} CH_2 \sim\sim$$

$$OH^- \downarrow$$

$$\sim\sim CH_2 \text{---} \overset{F}{\underset{OH}{C}} \text{---} CH = CF \text{---} CH_2 \sim\sim$$

Figure S7. The process of chemical reaction between PVDF and alkali.

This reaction causes hydrophilic hydroxyl groups to appear on the surface, reducing the hydrophobicity of the material. However, it has also been demonstrated that short-term immersion has little effect on the wettability of the material. In addition, in the process of separating heavy oil, a solid-gas-liquid interface or a solid-oil-water interface will be formed between the BTTM and the mixed liquid, which prevents the contact between the corrosion medium and the smart surface. Furthermore, considering its stability in acidic or salt solutions, the smart material is expected to be widely used in the recovery of industrial acidic oily wastewater.

Table S3. The water contact angles (WCAs) and sliding angles (WSAs) of the coated glass (H_2O as reference).

|	WCAs	WSAs
H_2O	148.6 ± 2.5°	40 ± 3°
2 M HCl	148.8 ± 3°	41 ± 3.5°
2 M NaOH	147.7 ± 2.5°	79 ± 4.5°
2 M NaCl	148.4 ± 3.5°	42 ± 2°
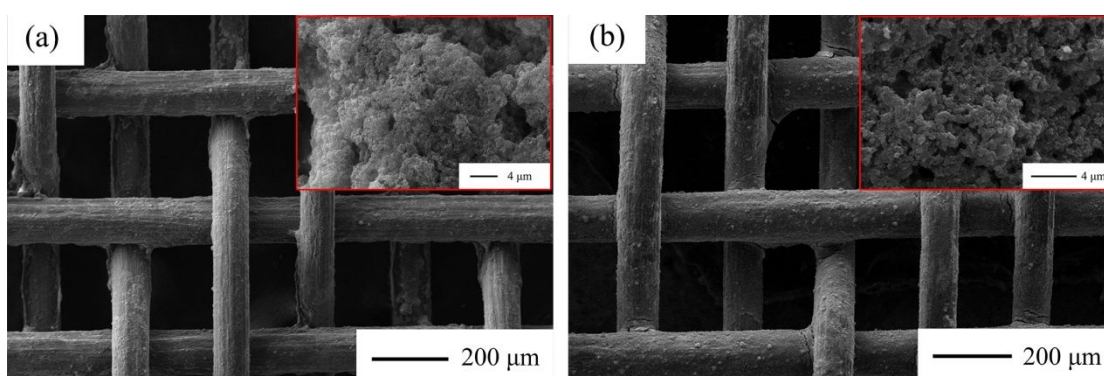
Figure S8. SEM images of the surfaces: (a) after immersing in alkaline solution for 12 hours and (b) immersed in liquid nitrogen for 1 hour.

The surface topography after immersion in the alkali solution for twelve hours compared to the original surface showed little change at low magnification (**Figure S**8a). However, at high magnification, many holes appeared on the surface after immersion, presumably due to the chemical reaction of PVDF with the alkali solution. Similarly, the surface topography after immersion in liquid nitrogen for 1 hour did not change much at low magnification compared to the original surface (**Figure S**8b). However, at high magnifications, there were also many holes in the surface. The holes

may be caused by irreversible damage during thermal expansion and contraction.
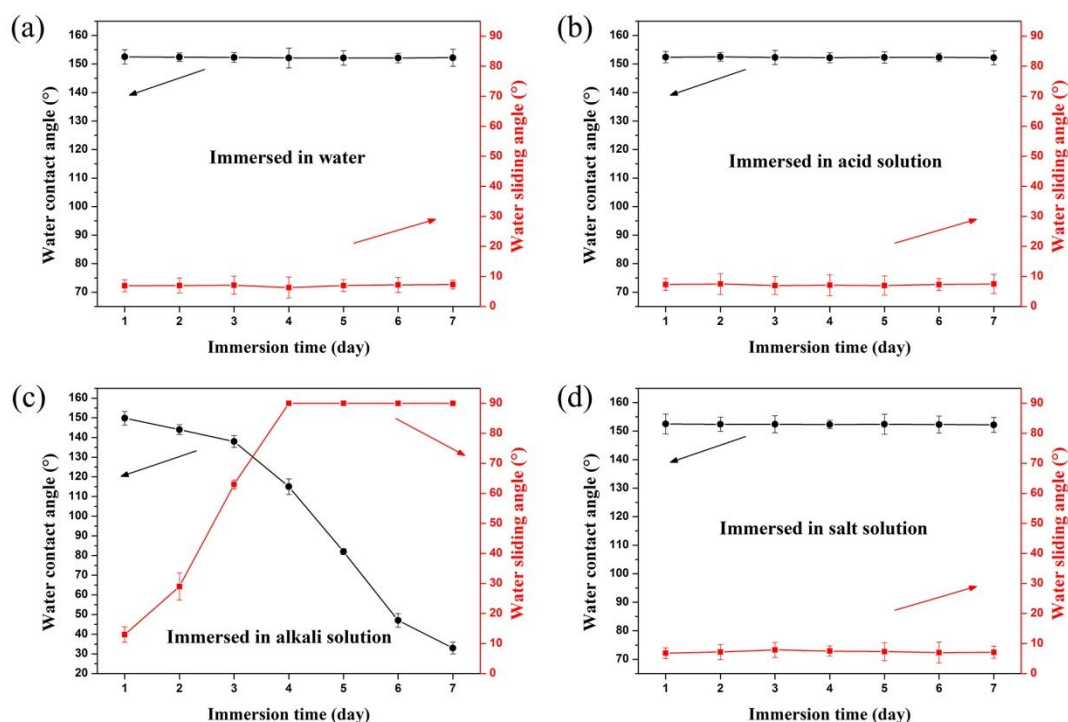
Figure S9. The change of WCAs and WSAs of the BTTM as a function of immersion time (immersed in water, acid solution (2 mol/L HCl), alkali solution (2 mol/L NaOH) and salt solution (2 mol/L NaCl)).

The immersion time was prolonged to further verify chemical stability of the BTTM. The results showed that the WCAs and WSAs of the BTTM were almost unchanged after immersion in water, acid solution and salt solution for seven days, showing excellent chemical stability. However, after immersing in an alkaline solution for seven days, the WCA was significantly reduced (33.0 ± 3 °) and the WSA was significantly increased (90 °). It can be attributed to the fact that PVDF can react with an alkaline solution to reduce surface energy (**Figure S7**). Nevertheless,

considering the large-scale emission of acidic oily wastewater in the industry, the as-prepared smart surface still has a good application prospect.
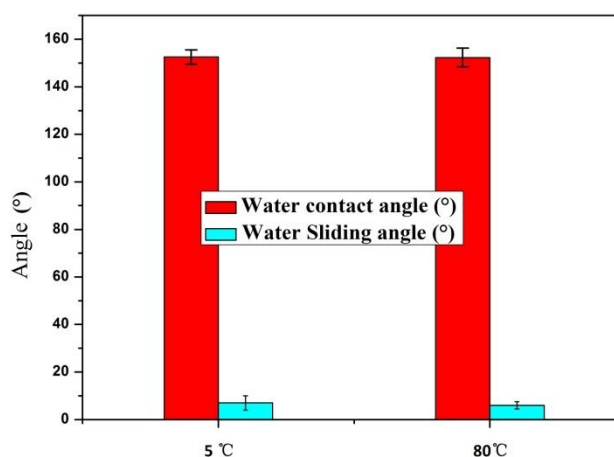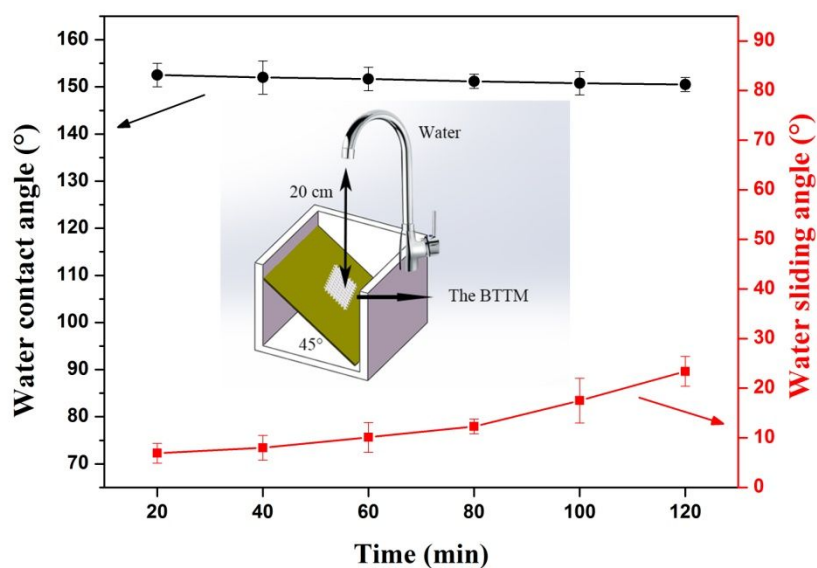

Figure S10. The WCAs and WSAs of as-prepared surface as a function of the different droplet temperature.

The WCAs and WSAs of as-prepared surface did not change significantly as the droplet temperature was raised (80 °C) or lowered (5 °C). It means that the material has good stability under the conditions of hot and cold liquid contact. This excellent stability extends the range of applications for the as-prepared surface.
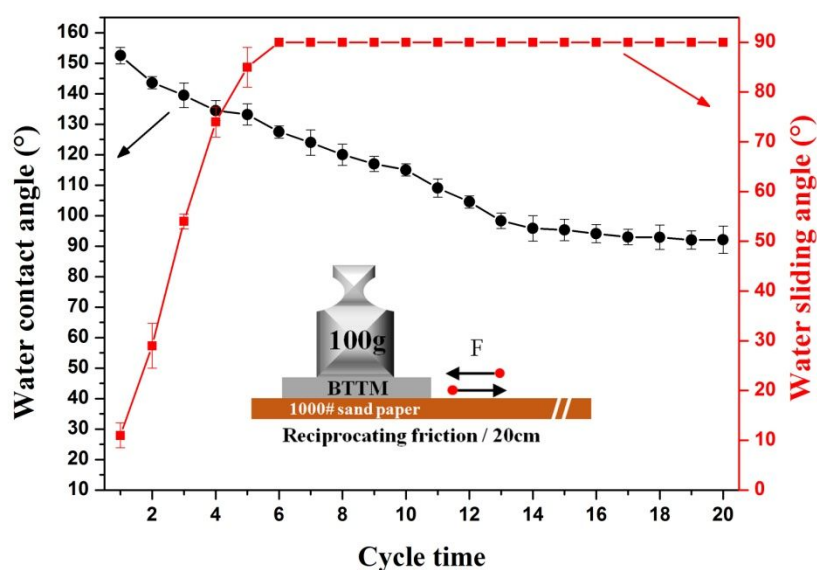
Figure S11. The WCAs of the as-prepared surface as a function of abrasion cycle, internal illustration is schematic of abrasion test.

The method of sandpaper abrasion was used to verify the mechanical stability of the surface. As shown in **Figure S**11, the WCA decreases significantly with the increase of wear cycle. After 20 times of friction, the WCA of the BTTM was 92.1 ± 4.5 ° and the WSA was 90°. It means that the surface is not good enough to resist physical damage. In further experiments, we consider adding epoxy resin to improve the adhesion between coating and surface. In addition, considering the use environment of membrane materials, we carried out water stream flushing experiment.

Figure S12. WCAs of as-prepared surface as a function of the different flushing time. Internal illustration is schematic illustration of water stream flushing experiment (the water outlet is 20 cm from the BTTM and the water flow rate is 1 m·s⁻¹.)

In order to further verify the stability of the surface, the water stream flushing experiment was carried out. Even after two hours of continuous impact of water flow, the surface still has a high contact angle (WCA was 150.5 ± 1.5 ° and WSA was 23.4 ± 3 °). Since the actual oil-water separation flow rate is much smaller than the flow rate of the water stream flushing experiment, the stability of the as-prepared surface can meet the actual needs.

Table S4. TiO_2 photocatalytic degradation of organic compounds.

Reactions
$TiO_2 + h\vartheta \rightarrow h^+ + e^-$
$OH^- + h^+ \rightarrow OH^c$
$O_2 + e^- \rightarrow O_2^-$
$H_2O \rightarrow OH^- + H^+$
$O_2^{\cdot -} + H^+ \rightarrow HOO^{\cdot}$
$HOO^{\cdot} + e^- \rightarrow HOO^-$
$HOO^- + H^+ \rightarrow H_2O_2$
$OH^{\cdot} + pollution + O_2^- \rightarrow CO_2, H_2O, etc.$